

Optimisation of neutron yield under ultra-intense laser impact on deuterated polyethylene targets

S.N. Andreev, S.G. Garanin, Yu.I. Yermicheva, A.A. Rukhadze, V.P. Tarakanov, B.P. Yakutov

Abstract. The modelling of interaction of ultra-intense femtosecond laser pulses with deuterated polyethylene targets is carried out with the processes of multiple field ionisation of the target atoms and the emission of neutrons produced in the course of the fusion reaction at high-energy deuteron collisions taken into account. The possibility of essential increase in the neutron yield (by tens of times) when using layered deuterated polyethylene targets with optimal dimensions of the layers and interlayer separations $\sim 1 \mu\text{m}$ is demonstrated.

Keywords: laser plasma, field ionisation, neutrons, layered target.

1. Introduction

Nuclear reactions occurring in targets with different composition under the action of ultra-intense laser pulses have been studied for more than a decade. As far back as in 1999, Russian scientists proposed a method of initiating nuclear reactions in the process of interaction of a high-power ultra-short laser pulse with plasma [1], and the nuclear reaction yield was estimated by using analytical calculations. In the same 1999 the paper [2] was published reporting the results of the first experiments on initiating photonuclear reactions by laser radiation using the British setup VULCAN.

The interest to this issue keeps high in recent years. Many experiments, aimed at the ignition of nuclear reactions using laser radiation (see, e.g., [3–5]), and theoretical studies of the relevant processes using analytical and numerical models (see, e.g., [6, 7]) have been carried out.

In the recent paper [8], devoted to numerical modelling of neutron emission in the fusion reaction $D(d,n)^3\text{He}$ (D–D reaction) under the irradiation of deuterated polyethylene targets with ultra-intense laser pulses, an approach was proposed, in which the probability of a D–D reaction event was calculated *ab initio* at each time step and for each deuteron in the process of self-consistent modelling of interaction between the laser pulse and the target using the PIC method. This approach was implemented within the framework of the relativistic electromagnetic PIC code KARAT [9, 10]. However, the process of multiple ionisation of the target was not taken into account.

S.N. Andreev, Yu.I. Yermicheva, A.A. Rukhadze, V.P. Tarakanov
A.M. Prokhorov General Physics Institute, Russian Academy of Sciences, ul. Vavilova 38, 119991 Moscow, Russia; e-mail: andreevsn@ran.gp.ru;
S.G. Garanin, B.P. Yakutov Russian Federal Nuclear Center ‘All-Russian Research Institute of Experimental Physics’ (RFNC–VNIIEF), prosp. Mira 37, 607183 Sarov, Nizhniy Novgorod region, Russia

Received 19 October 2011; revision received 21 February 2012
Kvantovaya Elektronika 42 (7) 600–604 (2012)
Translated by V.L. Derbov

In [8] a satisfactory agreement was obtained between the results of calculations and the known experimental data; it was also shown that the proposed method of neutron emission modelling allows investigation of layered targets, in which the neutron yield significantly increases. Obviously, the parameters of the target, such as its composition, the number of layers, their thickness, the separation between the layers essentially affect the acceleration of deuterons and neutron emission.

In the present paper we carry out the modelling of neutron emission at different parameters of the target aimed at optimising the parameters of the laser source of neutrons. In the course of modelling the process of multiple field ionisation of the target atoms under the laser impact is additionally taken into account.

2. Description of the model

For numerical modelling of the target ionisation dynamics at the initial stage of laser impact a special programme unit, describing the process of field ionisation, was developed and introduced into the PIC-code KARAT. The block describing the ionisation of atoms in the electromagnetic field of an intense femtosecond laser pulse is based on the Keldysh theory, thoroughly considered in the review [11]. The effect of tunnelling in the time-dependent electric field of the laser pulse and the multiphoton ionisation of atoms are two limiting cases of the nonlinear photoionisation process, the character of which essentially depends on the adiabaticity parameter (Keldysh parameter)

$$\gamma = \frac{1}{2K_0F}, \quad (1)$$

where $K_0 = I/(\hbar\omega)$; $F = E/(\chi^3 E_a)$; $\chi = [2I\hbar^2/(m_e e^4)]^{1/2}$; E is the electric field amplitude; ω is the frequency of the electric field; e is the electron charge; m_e is the electron mass; $E_a = m_e^2 e^5 / \hbar^4 = 5.14 \times 10^9 \text{ V cm}^{-1}$ is the atomic electric field strength; I is the ionisation potential of the atomic level. The tunnel ionisation of atomic states takes place in the case when $\gamma \lesssim 1$, whereas at $\gamma \gg 1$ the ionisation process is multiphoton [12]. At laser intensity higher than $10^{18} \text{ W cm}^{-2}$ the case $\gamma \ll 1$ takes place.

When $\gamma \ll 1$ and the polarisation of the electromagnetic wave is linear, the probability of ionisation of an atom (or ion) per unit time is determined by the formula [11]

$$W_{lm} = W_{l-m} = \frac{m_e e^4}{\hbar} \chi^2 \sqrt{\frac{3}{\pi}} (2l+1) \frac{(l+m)!}{2^m m!} \times C_{\chi l}^2 \cdot 2^{2n^* - m} F^{m+3/2-2n^*} \exp\left[-\frac{2}{3F} \left(1 - \frac{\gamma^2}{10}\right)\right], \quad (2)$$

where $m_e e^4 / \hbar = 4.13 \times 10^{16} \text{ s}^{-1}$; $m \geq 0$ is the absolute value of the quantum number, characterising the projection of the angular momentum l onto the axis, directed along the electric field; $n^* = Z/\chi$; Z is the charge of the atom (or ion);

$$C_{\chi l}^2 = \left| \frac{2^{2n^*-2}}{n^* \Gamma(n^* + l + 1) \Gamma(n^* - l)} \right|; \Gamma(n^* + 1) = n^*! \quad (3)$$

In the derivation of Eqn (2) the condition of multi-quantum process

$$K_0 = \frac{I}{\hbar \omega} \gg 1 \quad (4)$$

and the condition that the external electromagnetic field is small compared to the atomic field

$$F = \frac{E}{\chi^3 E_a} \ll 1 \quad (5)$$

were assumed to hold. For example, for laser radiation with the wavelength $\lambda = 1 \mu\text{m}$ ($\hbar\omega = 1.24 \text{ eV}$) and the electric field amplitude $E = E = 2.74 \times 10^{16} \text{ V cm}^{-1}$ (intensity $10^{18} \text{ W cm}^{-2}$) in the case of a hydrogen atom (ionisation potential $I = 13.6 \text{ eV}$) we have $K_0 = 11$ and $F = 5.3$. Therefore, for the considered parameters the condition (4) is obviously valid, while the condition (5) is not valid, since the amplitude of the laser pulse electric field is much greater than the atomic field E_a . In this case the probability of ionisation (2) is formally much greater than unity, which corresponds to instantaneous ionisation. However, with the growth of potential and multiplicity of ionisation in atoms having large charge number Z the quantity F decreases proportional to $I^{-3/2}$ and reaches unity at $I = 41 \text{ eV}$, thus satisfying both conditions (4) and (5).

The model of ionisation of atoms in the electromagnetic field of an intense laser pulse is implemented in the programme unit GFI (gas field ionisation), in which in the process of self-consistent modelling at each step in time and at each spatial point the probability of ionisation and electron-ion pair production, corresponding to the local gas density, is calculated, with the distribution of neutral atomic gas taken as the initial one. For the produced multiply charged ions at each time step for each individual particle the probability of its further ionisation is calculated in correspondence with the value of the electric field strength at the point of the particle location. If the probability is greater than the random number $0 < R < 1$, then the multiplicity of ionisation I of the particle is increased by unity and one more macro-electron is launched. Assuming that the modelling will be performed for the case of irradiating the gas with intense laser pulses, the macro-electrons are launched with zero initial momenta. The produced macro-particles then participate in the PIC-modelling on equal terms with all other participants of the ensemble.

The calculation domain, used to model the emission of neutrons under the action of ultra-intense laser pulse on the target, containing deuterium, was chosen to be a square with the dimensions of $20 \mu\text{m}$ along the axes x and z . The step of grid in both directions was 20 nm . The laser pulse was launched from the left boundary of the calculation domain and propagated in the positive direction of the z axis. The boundary conditions for electric and magnetic fields at the left and right boundaries of the calculation domain provided the input and output of the radiation. At the top and bottom boundaries of the calculation domain the boundary conditions

corresponded to an ideally conducting surface. For macro-particles all boundaries were absorbing.

The target was a layer of deuterated polyethylene $(\text{CD}_2)_n$ $l_0 = 4 \mu\text{m}$ thick and $d_0 = 16 \mu\text{m}$ wide, occupying the domain within $5 \leq z \leq 9 \mu\text{m}$ and $2 \leq x \leq 18 \mu\text{m}$. The ionisation of the target was modelled by means of the programme unit GFI, the initial concentration of deuterium atoms was $n_D = 8.22 \times 10^{22} \text{ cm}^{-3}$, and the concentration of carbon atoms was $n_C = 4.11 \times 10^{22} \text{ cm}^{-3}$, which corresponded to the solid-state density of deuterated polyethylene $\rho_{pe} = 1.105 \text{ g cm}^{-3}$.

In the ionisation programme unit the deuterium ionisation potential $I = 13.6 \text{ eV}$ was used, as well as the ionisation potentials of carbon atom, summarised in Table 1. The target was normally irradiated with a linearly polarised laser pulse with the following parameters: the wavelength $\lambda = 0.911 \mu\text{m}$, the Gaussian beam spot radius $r_0 = 3 \mu\text{m}$ centred at the point $x = 10 \mu\text{m}$, the pulse duration $\tau_0 = 45 \text{ fs}$. The intensity maximum of the laser pulse reached the front surface of the target at the moment of time $t = 61 \text{ fs}$. The maximal intensity of laser pulses varied within the range $I_0 = 10^{20} - 10^{21} \text{ W cm}^{-2}$.

Table 1. Parameters of multiple ionisation of a carbon atom.

| Ionisation multiplicity | Principal quantum number n | Angular momentum l | Projection of angular momentum m | Ionisation potential/eV |
|-------------------------|------------------------------|----------------------|------------------------------------|-------------------------|
| 1 | 2 | 1 | 0 | 11.3 |
| 2 | 2 | 1 | 1 | 24.4 |
| 3 | 2 | 0 | 0 | 47.9 |
| 4 | 2 | 0 | 0 | 64.5 |
| 5 | 1 | 0 | 0 | 392 |
| 6 | 1 | 0 | 0 | 490 |

3. Results of the calculations

The effect of a femtosecond pulse on the deuterated polyethylene target at the moment $t = 80 \text{ fs}$ is illustrated in Fig. 1.

The laser radiation, incident on the front surface of the target, causes ionisation of atoms in a thin near-surface layer as thick as the skin layer. The electrons produced in this pro-

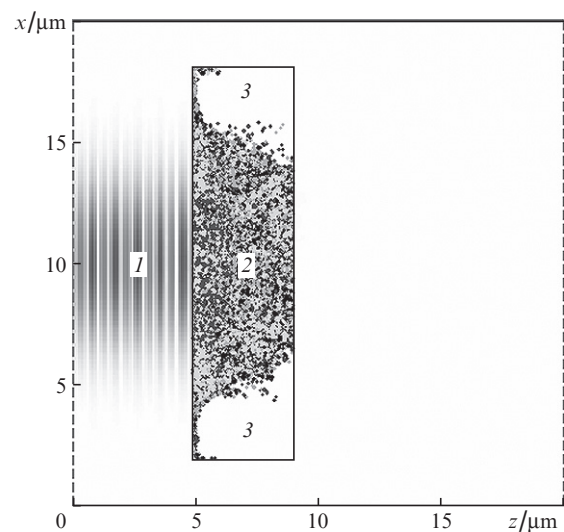


Figure 1. Impact of ultra-intense femtosecond laser pulse on the deuterated polyethylene target at the moment of time $t = 80 \text{ fs}$: (1) laser pulse; (2) multiply charged plasma; (3) the target regions not ionised to the considered moment of time.

cess are accelerated by the field of laser radiation and create an electric field of charge separation, which leads to propagation of the ionisation front into the target. In spite of the fact that the laser radiation does not penetrate deep into the target and is completely shielded by the surface layer of ionised substance, the entire target appears to be fully ionised. At the intensity of $I_0 = 10^{20} \text{ W cm}^{-2}$ the mean multiplicity of ionisation of the carbon atoms is equal to four, and at $I_0 = 10^{21} \text{ W cm}^{-2}$ it is equal to six. Obviously, the deuterium atoms are fully ionised.

As a result of the laser impact on the target, three fluxes of deuterons are produced, namely, the deuterons that move from the front surface of the target towards the laser pulse, the deuterons that move from the front surface into the target, and the deuterons that move from the back surface of the target in the direction of the laser pulse propagation.

Only a small fraction of deuterons is accelerated at the front and the back surface of the target, while the major part of deuterons within its volume remains cold. Moreover, only the deuterons moving from the front surface into the target can efficiently participate in D–D reactions with cold deuterons of the target, whereas the deuterons, moving off the target, in spite of their high energy, cannot significantly contribute to the neutron yield.

As the deuterons move through the target, the D–D reaction events occur, creating neutrons in correspondence with the model, thoroughly described in [8]. The probability of the fusion reaction event at each time step for each initial macroparticle, corresponding to a deuteron, was calculated using the formula

$$P = \sigma_{\text{dd}} |V_{\text{rel}}| n_{\text{d}} \Delta t, \quad (6)$$

where $\sigma_{\text{dd}}(E_0) = (107.4 + 0.33E_0)E_0^{-1} \exp(-44.4/\sqrt{E_0})$ is the cross section of the fusion $\text{D} + \text{D} \rightarrow {}^3\text{He} + \text{n}$ reaction (in barns); V_{rel} is the relative velocity of the initial deuteron and the random deuteron at the point of the initial deuteron location; n_{d} is the concentration of deuterons at this point; E_0 is the kinetic energy of the deuteron (in keV), corresponding to the velocity V_{rel} ; Δt is the time step.

The neutrons produced in the target volume began to reach the boundaries of the calculation domain in ~ 300 fs after the end of the laser action on the target. During 1 ps the neutron fluxes increased, reaching the maximum, and then decreased practically to zero during the next 1.5 ps.

Figure 2 presents the dependence of the total neutron yield (per 1 J of laser energy) on the intensity of the laser pulse. Curve (1) corresponds to the deuterated polyethylene target with the parameters, described above, and curve (2) corresponds to the target, containing only deuterium in the concentration, equal to that in the deuterated polyethylene target. The comparison of curves (1) and (2) shows that for the pure-deuterium target the neutron yield is 25–50 times higher than for the deuterated polyethylene target, i.e., the presence of carbon in the target leads to an essential reduction of the neutron yield.

Significant influence on the neutron yield is exerted by the process of field ionisation of the target. Indeed, curve (3), corresponding to the preliminarily ionised deuterated polyethylene target with double ionisation of carbon, shows that the neutron yield is overrated and nearly equals the neutron yield in the case of pure-deuterium target.

To clarify the mechanisms of the effect of carbon ions on the neutron yield we investigated the dependences of different

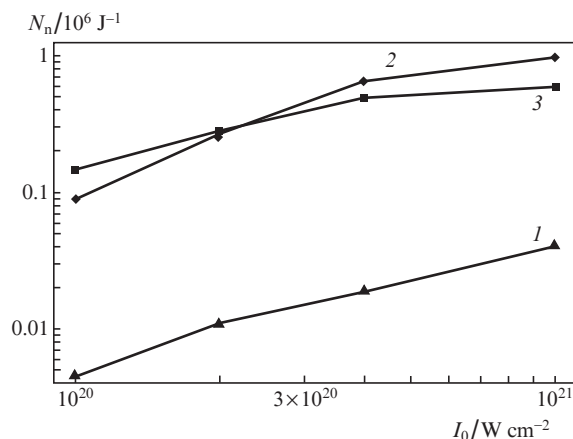


Figure 2. Dependence of the neutron yield per 1 J of laser radiation energy N_n on the maximal intensity of the laser pulse for the targets of $(\text{CD}_2)_n$ (1), D_2 (2), and pre-ionised $(\text{CD}_2)_n$ (3).

parameters of laser plasma on the concentration of carbon, the intensity of the laser pulse being fixed as $I_0 = 4 \times 10^{20} \text{ W cm}^{-2}$. It was found that the energy of laser radiation absorbed by electrons at the front surface of the target and transformed into the kinetic energy of the electrons is practically independent of the carbon concentration. Indeed, the fraction of the laser energy absorbed by electrons for the pure deuterium target ($n_{\text{C}} = 0$) amounts to 25.4%, and for the deuterated polyethylene target ($n_{\text{C}} = 4.11 \times 10^{22} \text{ cm}^{-3}$) 24.6%. In the pure deuterium target the total number of electrons is four times smaller than in the deuterated polyethylene target. As a result the maximal mean energy of electrons and, as a consequence, the maximal kinetic energy of deuterons for the pure deuterium target appears to be greater than for the deuterated polyethylene target. Figures 3 and 4 show the dependences of the maximal mean energy of electrons and the maximal kinetic energy of deuterons, respectively, scaled to the laser pulse energy, on the concentration of carbon atoms in the target. It is seen that these energies in the case of pure deuterium target are by 4.4 times greater than in the case of the deuterated polyethylene target. The neutron yield in this case increases by 4 times (see Fig. 2).

Thus, to increase the neutron yield one should prefer such solid-state targets, in which the concentration of deuterium atoms is maximal [see Eqn (6)], and the number of electrons,

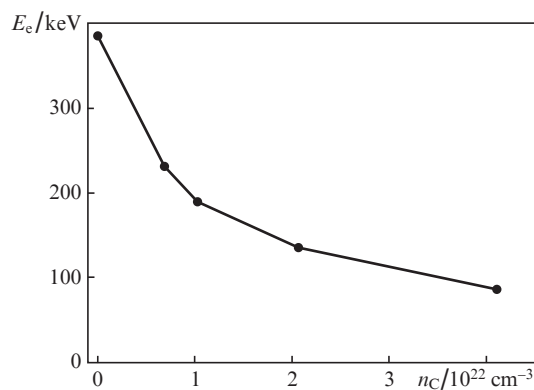


Figure 3. Dependence of the maximal mean energy of electrons E_e on the concentration of carbon atoms.

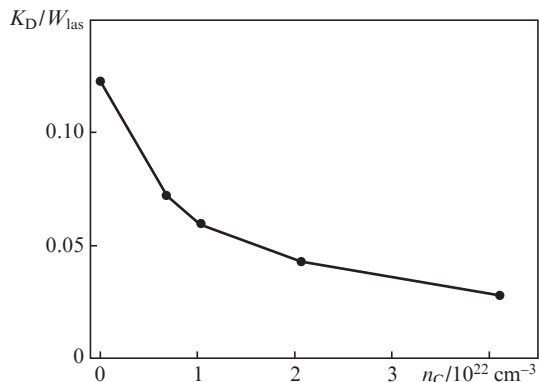


Figure 4. Dependence of the ratio of maximal kinetic energy of deuteron K_D to the total energy of the laser pulse W_{las} on the concentration of carbon atoms.

with the multiple ionisation of target atoms taken into account, is minimal (which provides their maximal energy). From this point of view the targets made of lithium deuteride LiD seem most promising. In these targets the concentration of deuterons ($n_D = 6.13 \times 10^{22} \text{ cm}^{-3}$) is 1.34 times smaller than in deuterated polyethylene targets, the maximal concentration of electrons at total ionisation of the target being also 1.34 times smaller. One can expect that, at other conditions being equal, the maximal energy of electrons in lithium deuteride targets will be considerably higher than in the deuterated polyethylene targets. Detailed comparison of lithium deuteride targets and deuterated polyethylene ones, as well as other targets having different composition, will be carried out in our future publications.

An additional possibility to increase the neutron yield under the conditions of ultra-intense laser irradiation of the targets, containing deuterium, consists in using the targets with complex shape, in particular, the layered ones. Under irradiation of a layered target, the deuteron fluxes, analogous to the three ones described above, are produced in each of the layers. Such a redistribution of the fluxes leads to a considerable increase of the number of accelerated deuterons, moving in opposite directions inside the layered target, and to the growth of the neutron yield. We performed calculations, in which the parameters of the laser pulse and the target were exactly corresponding to the case, considered above ($n_C = 4.11 \times 10^{22} \text{ cm}^{-3}$) except the target being divided into similar parts, separated by equal distances from each other. The intensity of the laser pulse was $I_0 = 4 \times 10^{20} \text{ W cm}^{-2}$.

Figure 5 shows the dependence of neutron yield per 1 J of laser energy on the number of layers in the deuterated polyethylene target. The following schemes of dividing the target into layers were considered: one layer 4 μm thick with the density ρ_{pe} ; two layers 2 μm thick with the density ρ_{pe} separated by 2 μm ; four layers 1 μm thick with the density ρ_{pe} , separated by 0.5 μm ; eight layers 2 μm thick with the density ρ_{pe} , separated by 0.5 μm ; sixteen layers 0.25 μm thick with the density ρ_{pe} , separated by 0.25 μm ; thirty two layers 0.125 μm thick with the density ρ_{pe} , separated by 0.125 μm ; one layer 8 μm thick with the density $0.5\rho_{\text{pe}}$, corresponding to an infinite number of layers with the thickness tending to zero. The mean density of the targets averaged over the thickness of 8 μm in all seven cases was equal $0.5\rho_{\text{pe}}$.

From Fig. 5 it is seen that the presence of even two layers in the target causes the increase in the neutron yield by almost

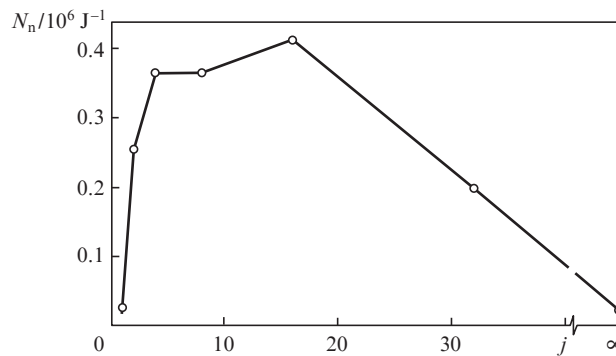


Figure 5. Dependence of the neutron yield per 1 J of laser radiation energy N_n on the number of layers in the target j .

14 times ($N_n = 225000$) per 1 J of laser energy as compared with the single-layer target 4 μm thick with the density ρ_{pe} ($N_n = 18800$). The maximal number of neutrons $N_n = 413000$ was achieved for the target with 16 layers separated by 0.25 μm from each other. Further increase in the number of layers and decreasing the separation between them leads to gradual lowering of the neutron yield. In the limit of infinite number of layers (one layer 8 μm thick with the density $0.5\rho_{\text{pe}}$) the neutron yield was reduced to $N_n = 22600$.

To explain this dependence, consider the distribution of the z -component of the charge separation electric field in a layered target. This field is a superposition of electric fields of each layer. Figures 6 and 7 show the distributions of the z -component of the electric field for targets, consisting of 16 and 32 layers, respectively, at the moment of time $t = 200 \text{ fs}$. The electric field distribution possesses bipolar shape with negative and positive extrema at the left and the right boundaries of the layer, respectively. In the regions corresponding to the field extrema the acceleration is most efficient and the deuteron fluxes, directed from the layer boundaries, are produced. If the interlayer separation is reduced, then the electric fields, created at the left and the right boundaries of the adjacent layers (except the leftmost and the rightmost layers) begin to overlap and mutually compensate (Fig. 7). As a result, the efficiency of the deuteron acceleration inside the layered

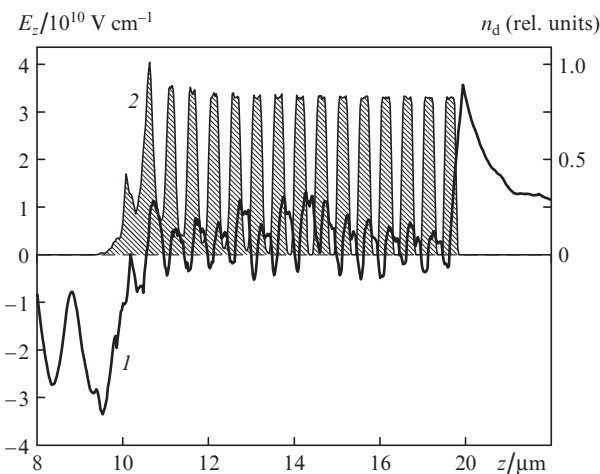


Figure 6. Distribution of the electric field component E_z (1) and the concentration of deuterons n_d (2) in the target, comprising 16 layers, at the moment of time $t = 200 \text{ fs}$.

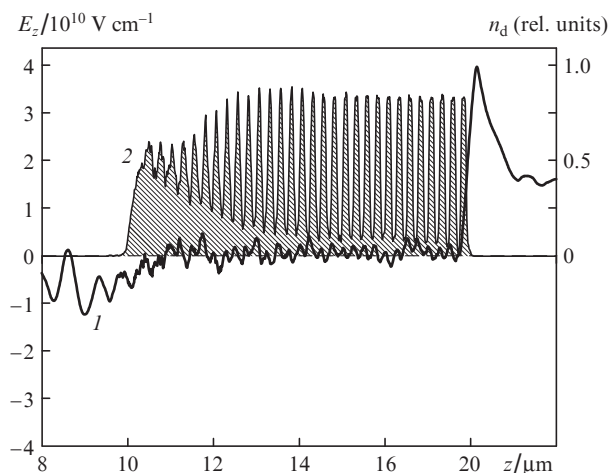


Figure 7. Distribution of the electric field component E_z (1) and the concentration of deuterons n_d (2) in the target, comprising 32 layers, at the moment of time $t = 200$ fs.

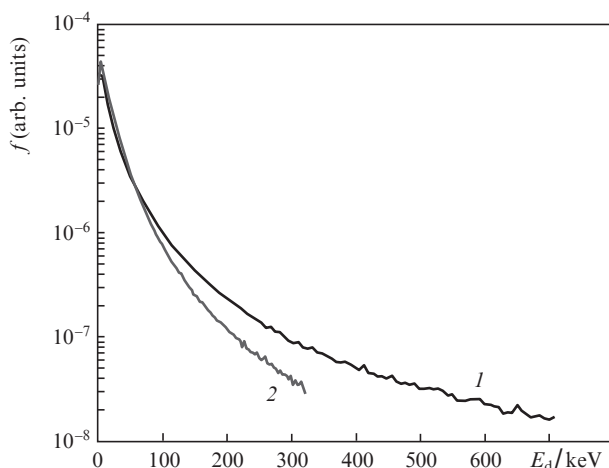


Figure 8. Energy spectra of deuterons in the targets with 16 (1) and 32 (2) layers at the moment of time $t = 1$ ps.

target decreases, which leads to the reduction of the neutron yield. This conclusion is confirmed by Fig. 8, in which the energy spectra of deuterons are presented for the targets with 16 and 32 layers at the time moment $t = 1$ ps under irradiation with a laser pulse with the intensity $I_0 = 4 \times 10^{20} \text{ W cm}^{-2}$. It is seen that the maximal energy of high-energy deuterons in the 16-layer target is more than two times higher than that in the 32-layer target. Besides that, the number of deuterons with the energy, exceeding 100 keV, in the 16-layer target is two times greater than in the 32-layer one.

From Fig. 5 it is also seen that the dependence of the neutron yield on the number of target layers (and the separation between them) is rather weak. Of crucial importance is the presence of cavities in the target, at the boundaries of which multidirectional fluxes of accelerated deuterons arise. Therefore, to provide an essential increase in the neutron yield under the conditions of irradiating solid-state targets with ultra-intense femtosecond laser pulses, it seems reasonable to use layered or porous targets having the typical cavity size of $\sim 1 \mu\text{m}$.

4. Conclusions

In the present paper the modelling of interaction of ultra-intense femtosecond laser pulses with solid-state deuterated polyethylene targets is carried out, taking into account the processes of multiple field ionisation of the target atoms and the emission of neutrons, produced in the fusion reaction, when high-energy deuterons collide.

It is shown that the ionisation of atoms in the volume of the target, to which the incident radiation does not penetrate, is provided by the electric field of charge separation, arising at the expansion of electrons, accelerated by the laser pulse at the front surface of the target.

The characteristics of the target hot plasma and the neutron yield are investigated depending on the concentration of carbon atoms in the target. It is found that in order to increase the neutron yield it is preferable to use such solid-state targets, in which the concentration of deuterium atoms is maximal and the number of electrons, with the multiple ionisation of the target atoms taken into account, is minimal.

The possibility is demonstrated to increase the neutron yield essentially (by tens of times) by using layered targets, made of deuterated polyethylene and irradiated with ultra-intense femtosecond laser pulses. The dependence of the neutron yield on the number of layers and the separation between them is studied. It is shown that this dependence is rather weak and the crucial role is played by the presence of sub-micron-size cavities in the volume of the target. At the boundaries of such cavities multidirectional fluxes of accelerated deuterons arise. The collisions of these deuterons with each other and with resting deuterons of the target essentially increase the total neutron yield.

Acknowledgements. The work was supported by the Grant of the President of the Russian Federation for State Support of Young Russian Scientists (Grant No. MK-1117.2012.2).

References

1. Bychenkov V.Yu., Tikhonchuk V.T., Tolokonnikov C.V. *Zh. Eksp. Teor. Fiz.*, **88**, 2080 (1999) [*JETP*, **88**, 1137 (1999)].
2. Ledingham K.W.D., Norreys P.A. *Contemp. Phys.*, **40**, 367 (1999).
3. McKenna P. *Proc. 11th Int. Conf. on Emerging Nuclear Energy Systems* (Albuquerque, USA, 2002).
4. McKenna P., Ledingham K.W.D., Robson L. *Lect. Notes Phys.*, **694**, 91 (2006).
5. Higgison D.P. *Phys. Plasmas*, **18**, 100703 (2011).
6. Macchi A. *Appl. Phys. B*, **82**, 337 (2006).
7. Petrov G.M., Davis J. *Phys. Plasmas*, **15**, 073109 (2008).
8. Andreev S.N., Garanin S.G., Rukhadze A.A., Tarakanov V.P., Yakutov B.P. *Kvantovaya Elektron.*, **41**, 377 (2011) [*Quantum Electron.*, **41**, 377 (2011)].
9. Tarakanov V.P. *User's Manual for Code KARAT* (VA, USA: Berkeley Research Associates, Inc., 1992).
10. Andreev S.N., Garanin S.G., Rukhadze A.A., Tarakanov V.P., Yakutov B.P. *Kvantovaya Elektron.*, **40**, 355 (2010) [*Quantum Electron.*, **40**, 355 (2010)].
11. Popov V.S. *Usp. Fiz. Nauk*, **174**, 921 (2004) [*Phys.-Usp.*, **47** (9), 855 (2004)].
12. Keldysh L.V. *Zh. Eksp. Teor. Fiz.*, **47**, 1945 (1964) [*Sov. Phys. JETP*, **20** (5), 1307 (1965)].